

Supporting Information

Table of Contents

Experimental Section	S2
Table S1: Crystallographic data and structure refinements for 1Er and 2Er	S5
Table S2: Selected bond lengths and angles of 1Er and 2Er	S6
Table S3: Kramers doublets (KDs) energy spectrum (cm^{-1}) and g tensors of the ground states for 1Er and 2Er	S7
Table S4: Kramers doublets (KDs) energy spectrums (cm^{-1}) and g tensors corresponding to modified 1Er	S8
Figure S1: $\chi_m T$ vs T plots.....	S9
Figure S2: Hysteresis under different field-sweeping rates for 1Er at 2 K.....	S10
Figure S3: Temperature dependence ac susceptibilities for 1Er	S11
Figure S4: Frequency-dependent out-of-phase susceptibilities for 1Er	S12
Figure S5: Cole-Cole plots for 1Er	S13
Figure S6: Frequency-dependent out-of-phase susceptibilities for 2Er	S14
Figure S7: Cole-Cole plots for 2Er	S15
Figure. S8 <i>Ab initio</i> calculated easy axis for 1Er	S16
Figure. S9 <i>Ab initio</i> calculated easy axis for 2Er	S17
Figure. S10 The blocking barriers for 1Er (a) and 2Er (b).....	S18
Figure S11: Near-IR emissive spectra of 1Er at 77 K.....	S19

Experimental Section

The synthesis of air and/or moisture sensitive compounds was carried out under an atmosphere of argon using Schlenk techniques or in an Argon filled glovebox. THF was dried in solvent purification system, transferred under vacuum, and stored in the glovebox. Cyclooctatetraene (COT) was degassed after dried over activated 4 Å molecular sieves overnight. [(COT)ErCl(THF)_x] was prepared according to literature procedures.¹ Unless otherwise noted, all starting materials were commercially available and were used without further purification. Elemental analysis was performed by Elementar Vario MICRO CUBE (Germany).

1Er [(LOMe)Er(COT)] (LOMe: (cyclopentadienyl)tris(di(methyl)phosphito)cobaltate): A THF solution (3 mL) of LOMeNa (237 mg, 0.5 mmol) was slowly added to the slurry of [(COT)ErCl(THF)_x] (189 mg, 0.5 mmol) in THF and stirred overnight. The solution was filtered and solvent was removed under vacuum. The residue was redissolved in toluene and stored in -25°C. Red crystals were obtained suitable for X-ray diffraction analysis after two days. Anal. Calcd (%) for C₁₉H₃₁CoErO₉P₃: C, 31.48; H, 4.32. Found: C, 31.00; H, 4.15.

2Er [(ArO)Er(COT)] (Ar = -C₆H₃-2,6-(2',6'-iPr₂C₆H₃)₂): KOAr was prepared from ArOH and KH in toluene in a quantitative yield according to literature.² In a glovebox KOAr (45.3 mg, 0.10 mmol) was mixed with COTErCl(thf)_x (75.4 mg, ca. 0.2 mmol) in a Schlenk tube. When THF (ca. 10 mL) was added to the mixture and stirred at room temperature a suspension formed. This Schlenk tube was sealed and taken outside of the glovebox. Then it was warmed to 90 °C in an oil bath and stirred for 12 h. When it cooled to room temperature this Schlenk tube was taken inside the glovebox. The solution was concentrated to ca. 1.5 mL and then filtered. The pink crystals of **2Er** can be obtained from its THF/hexane solution. Anal. Calcd (%) for C₄₆H₆₁ErO₃: C, 66.63; H, 7.41. Found: C, 66.35; H, 7.51.

X-ray crystallography and magnetic measurement

All crystals were manipulated under a nitrogen atmosphere and were covered in grease. Data collections were performed at 180 K on a Aglient technologies Super Nova Atlas Dual System, with a (Mo $K\alpha = 0.71073 \text{ \AA}$) microfocus source and focusing multilayer mirror optics. The structures were solved with the Superflip structure solution program using Charge Flipping and refined with the XL refinement package using Least Squares minimization that implanted in Olex2.^{2,3} All non-hydrogen atoms were refined anisotropically. Hydrogen atoms were placed at the calculation positions.

Samples were fixed by N-grease to avoid moving and decaying during measurement. Direct current susceptibility experiment was performed on Quantum Design MPMS XL-5 SQUID magnetometer on polycrystalline samples. Alternative current susceptibility measurement with frequencies ranging from 100 Hz to 10000 Hz was performed on Quantum Design PPMS on polycrystalline samples. All dc susceptibilities were corrected for diamagnetic contribution from the sample holder, N-grease and diamagnetic contributions from the molecule using the pascal's constants.

***Ab initio* calculations**

Complete-active-space self-consistent field (CASSCF) calculations on the complete structures of complexes **1Er** and **2Er** on the basis of X-ray determined geometry have been carried out with MOLCAS 8.0 program package.⁴ For CASSCF calculations, the basis sets for all atoms are atomic natural orbitals from the MOLCAS ANO-RCC library: ANO-RCC-VTZP for Er^{III} ion; VTZ for close C and O; VDZ for distant atoms. The calculations employed the second order Douglas-Kroll-Hess Hamiltonian, where scalar relativistic contractions were taken into account in the basis set and the spin-orbit coupling was handled separately in the restricted active space state interaction (RASSI-SO) procedure. The active electrons in 7 active spaces included all f electrons (CAS(11 in 7)) in the CASSCF calculation. To exclude all the doubts we calculated all the roots in the active space. We have mixed the maximum number of spin-free states which

was possible with our hardware (all from 35 quadruplets and all from 112 doublets).

Near-IR emission spectrum measurement.

Steady state emission spectra was acquired on an Edinburgh Analytical Instruments FLS920 lifetime and steady-state spectrometer (450 W Xe lamp, Ge detector for NIR emission spectrum, Hamamatsu R5509-73 PMT with C9940-02 cooler) on frozen glasses of solutions of the **1Er** (2-methyl-tetrahydrofuran) using a dewar cuvette filled with liquid N₂ (T = 77 K).

References

- 1) H. Schumann, R. D. Koehn, F. W. Reier, A. Dietrich and J. Pickardt, *Organometallics*, 1989, **8**, 1388.
- 2) a) Sheldrick, G. M. A short history of SHELX. *Acta Cryst.* 2008, **A64**, 112-122; b) Dolomanov, O. V.; Bourhis, L. J.; Gildea, R. J.; Howard, J. A. K.; Puschmann, H. OLEX2: a complete structure solution, refinement and analysis program. *J. Appl. Crystallogr.* 2009, **42**, 339; c) Palatinus, L.; Chapuis, G. SUPERFLIP– a computer program for the solution of crystal structures by charge flipping in arbitrary dimensions. *J. Appl. Crystallogr.*, 2007, **40**, 786-790.
- 3) Spek, A. L. *Acta Cryst.*, 2009, **D65**, 148.
- 4) C. Stanciu, M. M. Olmstead, A. D. Phillips, M. S., P. P. Power, *Eur. J. Inorg. Chem.*, 2003, **2003**, 3495.
- 5) a) F. Aquilante, J. Autschbach, R. K. Carlson, L. F. Chibotaru, M. G. Delcey, L. De Vico, I. Fdez. Galván, N. Ferré, L. M. Frutos, L. Gagliardi, M. Garavelli, A. Giussani, C. E. Hoyer, G. Li Manni, H. Lischka, D. Ma, P. Å. Malmqvist, T. Müller, A. Nenov, M. Olivucci, T. B. Pedersen, D. Peng, F. Plasser, B. Pritchard, M. Reiher, I. Rivalta, I. Schapiro, J. Segarra - Martíde, M. Stenrup, D. G. Truhlar, L. Ungur, A. Valentini, S. Vancoillie, V. Veryazov, V. P. Vysotskiy, O. Weingart, F. Zapata, R. Lindh, *J. Comput. Chem.*, 2016, **37**, 506; b) L. Ungur, M. Thewissen, J.-P. Costes, W. Wernsdorfer, L. F. Chibotaru, *Inorg. Chem.*, 2013, **52**, 6328.

Table S1 Crystallographic data and structure refinements for **1Er** and **2Er**.

formula	C ₁₉ H ₃₁ CoErO ₉ P ₃	C ₄₆ H ₆₁ ErO ₃
Mr	722.54	570.27
cryst syst	orthorhombic	orthorhombic
space group	<i>Pnma</i>	<i>P2₁2₁2₁</i>
<i>a</i> , Å	20.9027(2)	12.4119(3)
<i>b</i> , Å	11.96320(14)	16.2512(4)
<i>c</i> , Å	22.3054(2)	20.0292(5)
<i>V</i> , Å ³	5577.75(11)	4040.05(18)
<i>α</i> , deg	90	90
<i>β</i> , deg	90	90
<i>γ</i> , deg	90	90
<i>Z</i>	8	4
<i>T</i> , K	180(2)	180(2)
<i>μ</i> , mm ⁻¹	3.797	2.115
<i>λ</i> , Å	0.71073	0.71073
Cryst size, mm ³	0.31*0.18*0.11	0.3*0.15*0.15
GOF	1.091	1.050
<i>R</i> _{int}	0.0424	0.0408
<i>R</i> ₁ , <i>wR</i> ₂ [<i>I</i> > 2σ(<i>I</i>)]	0.0481, 0.1545	0.0281, 0.0486
<i>R</i> ₁ , <i>wR</i> ₂ [all data]	0.0569, 0.1637	0.0387, 0.0530
CCDC code	1900286	1900287

Table S2 Selected bond lengths and angles of **1Er** and **2Er**.

	1Er(A)	1Er(B)	2Er
Er–O(1), Å	2.236	2.231	2.409
Er–O(2), Å	2.236	2.231	2.428
Er–O(3), Å	2.245	2.256	2.132
Er–C(COT), Å	2.564-2.585	2.550-2.586	2.555-2.573
Er–centroid (COT), Å	1.805	1.802	1.826
Er–centroid (O), Å	1.489	1.477	1.498
∠O(1)-Er-O(2), °	81.5	82.3	76.0
∠O(2)-Er-O(3), °	80.1	80.7	86.8
∠O(3)-Er-O(1), °	80.1	80.7	86.8
∠centroid (O)-Er-centroid (COT), °	176.4	176.7	163.3
Dihedral angle, °	4.8	5.1	3.7

Table S3 Kramers doublets (KDs) energy spectrums (cm^{-1}) and g tensors of the ground states

	1Er	2Er
	Kramers doublets (KDs) energy spectrum	
1	0	0
2	111.6	55.5
3	199.4	94.8
4	223.6	138.1
5	227.4	236.4
6	268.2	261.3
7	290.0	304.3
8	300.7	396.5
	g tensor of the ground state	
g_x	1×10^{-5}	0.0595
g_y	1×10^{-5}	0.0960
g_z	17.92	17.44

Table S4 Kramers doublets (KDs) energy spectrums (cm^{-1}) and g tensors corresponding to modified **1Er**.

KDs	Er–Centroid (O): 1.389 Å			Er–Centroid (O): 1.589 Å		
	E			E		
1	0			0		
2	113.6			114.2		
3	198.4			223.3		
4	224.0			231.7		
5	227.5			250.1		
6	268.0			288.4		
7	291.2			303.2		
8	300.9			317.0		
KDs	g_x	g_y	g_z	g_x	g_y	g_z
1	2.018E-5	2.808E-5	17.9211	1.146E-5	1.418E-5	17.9362
2	0.0051	0.0053	15.4853	0.0018	0.0019	15.5167
3	9.8248	9.3993	1.1648	9.8254	9.15082	0.9802
4	0.2319	0.5468	9.2977	0.0112	0.3389	12.774
5	0.3942	0.7952	7.4455	0.1871	0.8465	3.6579
6	0.1508	0.8837	6.6792	0.2514	0.8234	6.6989
7	0.0154	0.3290	10.6106	0.0223	0.2775	10.3896
8	0.25255	0.8053	10.4391	0.3715	0.7654	9.5182
KDs	Er–Centroid (O): 1.689 Å			Er–Centroid (O): ∞		
	E			E		
1	0			0		
2	108.3			140.0		
3	206.1			305.1		
4	222.9			428.7		
5	233.5			485.3		
6	273.6			492.1		
7	291.3			498.2		
8	304.1			507.8		
KDs	g_x	g_y	g_z	g_x	g_y	g_z
1	8.403E-6	9.442E-6	17.9451	2.38E-7	4.77E-7	17.9510
2	0.0011	0.0011	15.5314	5.255E-5	5.287E-5	15.5418
3	10.2876	8.9837	1.1714	4.971E-4	5.074E-4	13.1275
4	0.0117	0.0578	13.0222	0.0161	0.0165	10.7333
5	0.5148	0.8811	3.6421	12.1359	7.1011	1.1427
6	0.3266	0.6357	6.4768	0.94603	1.22719	7.95135
7	0.0195	0.1366	10.5757	3.89918	2.88171	1.79195
8	0.2922	0.5939	10.1354	0.56614	1.24625	5.97921

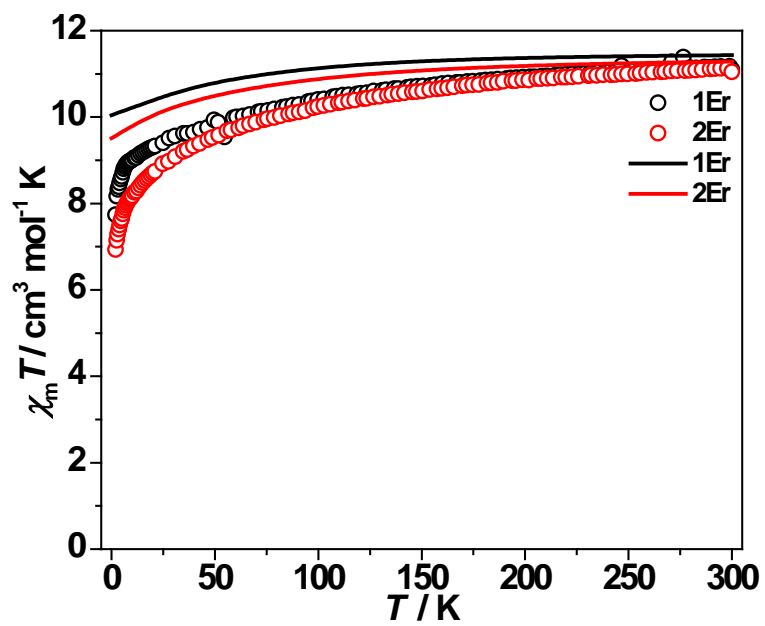


Fig. S1 $\chi_m T$ vs T plots for **1Er** (black circles) and **2Er** (red circles). The solid lines represent the *ab initio* calculated results.

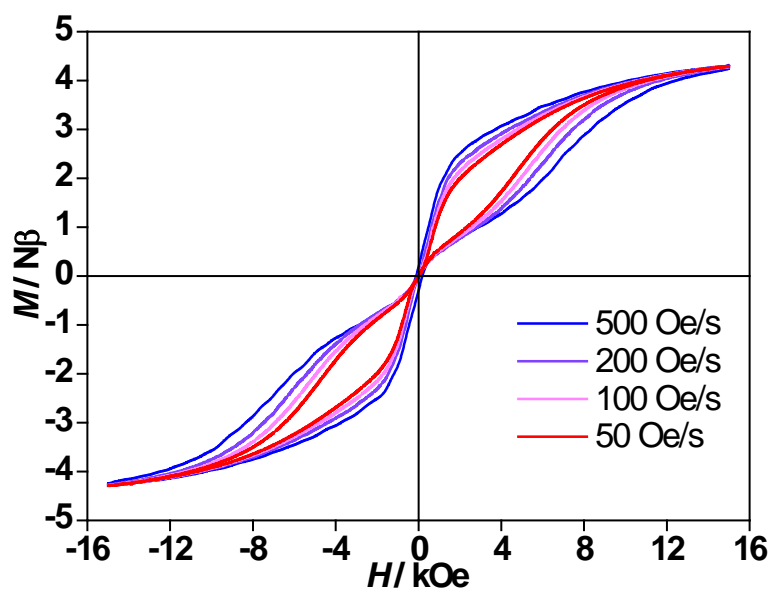


Fig. S2 Hysteresis measurement under different field sweeping rates for **1Er** at 2 K.

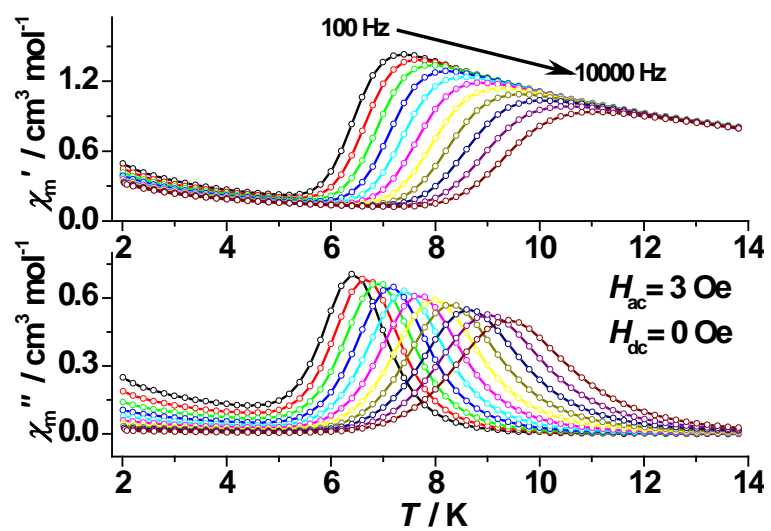


Fig. S3 Temperature dependence ac susceptibility in the absence of dc field for **1Er**.

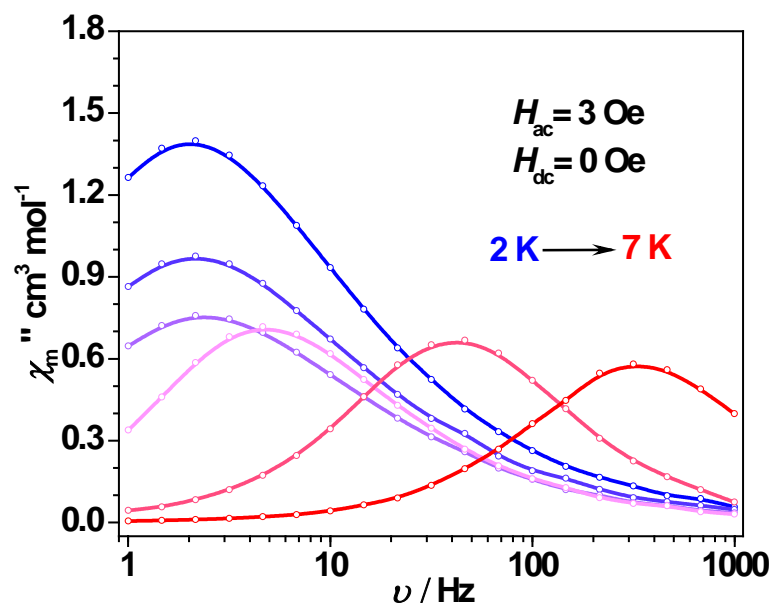
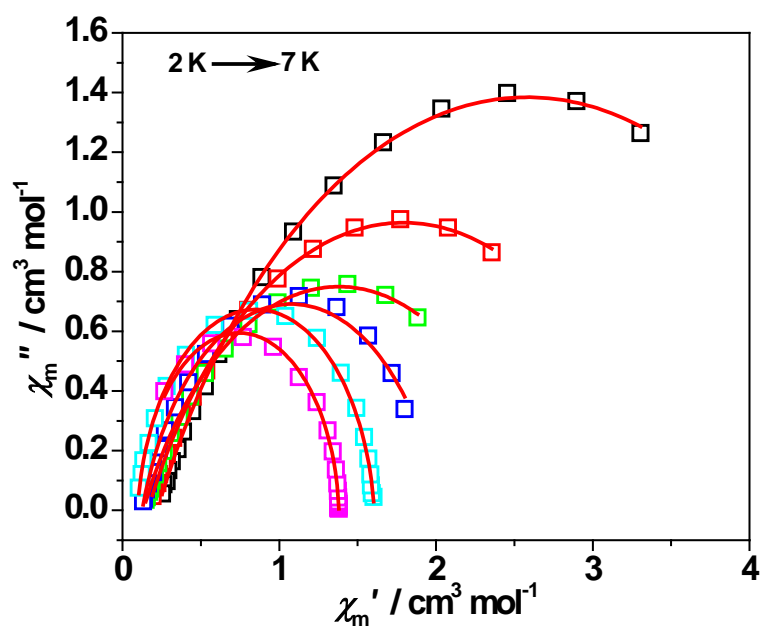


Fig. S4 Frequency-dependent out-of-phase susceptibilities for **1Er**.

(a)



(b)

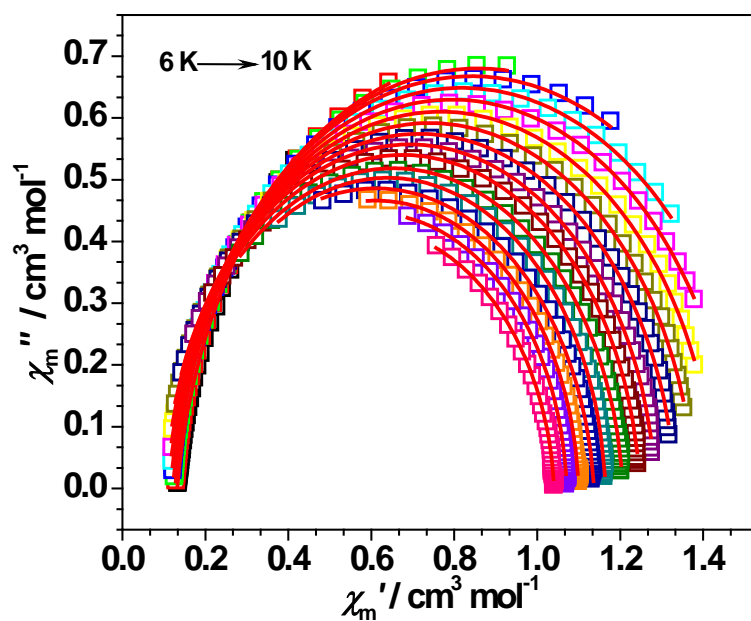
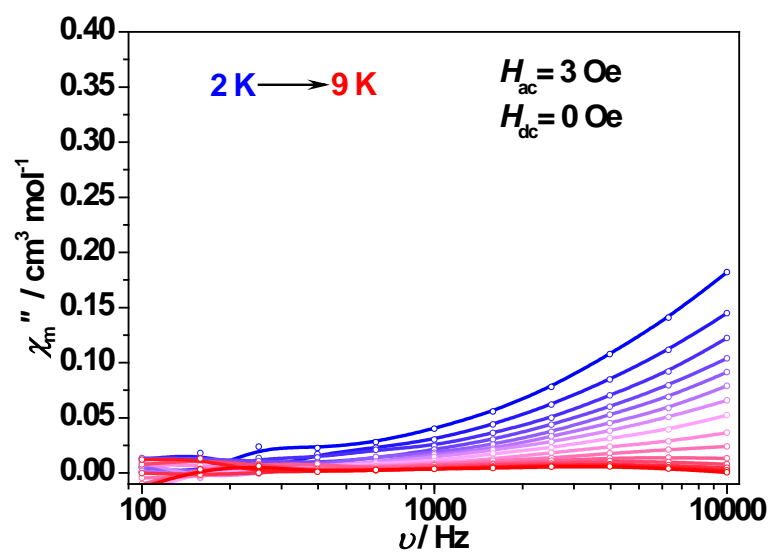


Fig. S5 Cole-Cole plots fitted by utilizing generalized Debye model for **1Er**. (a) presents the data from MPMS in the frequency range of 1-1000 Hz. (b) represents the data from PPMS in the frequency range of 100-10000 Hz.

(a)



(b)

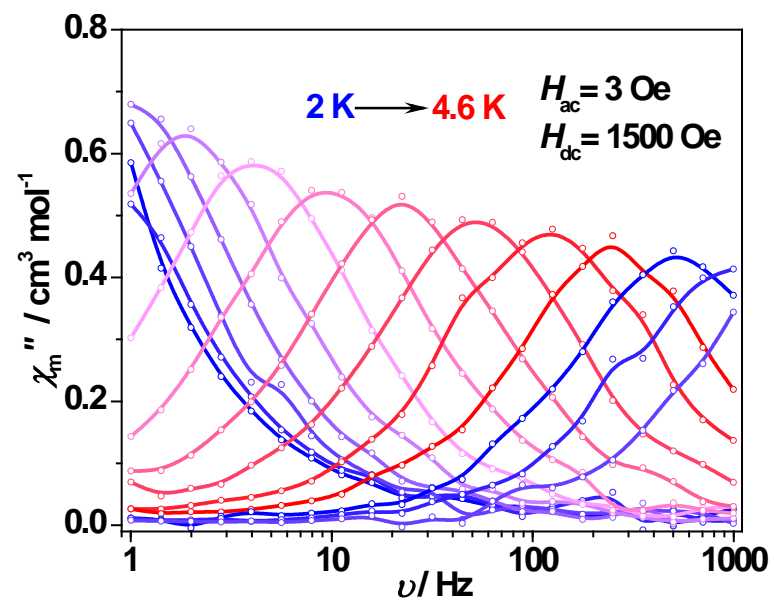
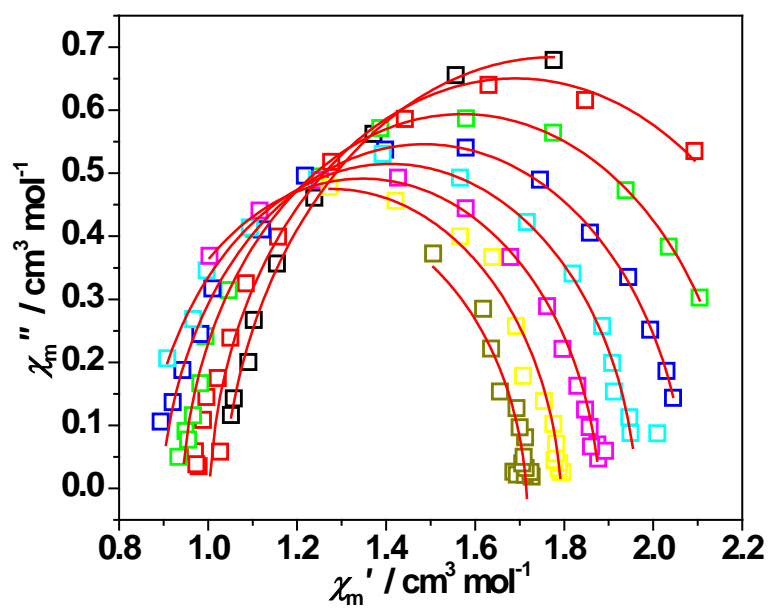


Fig. S6 Frequency-dependent out-of-phase susceptibilities for **2Er**.

(a)



(b)

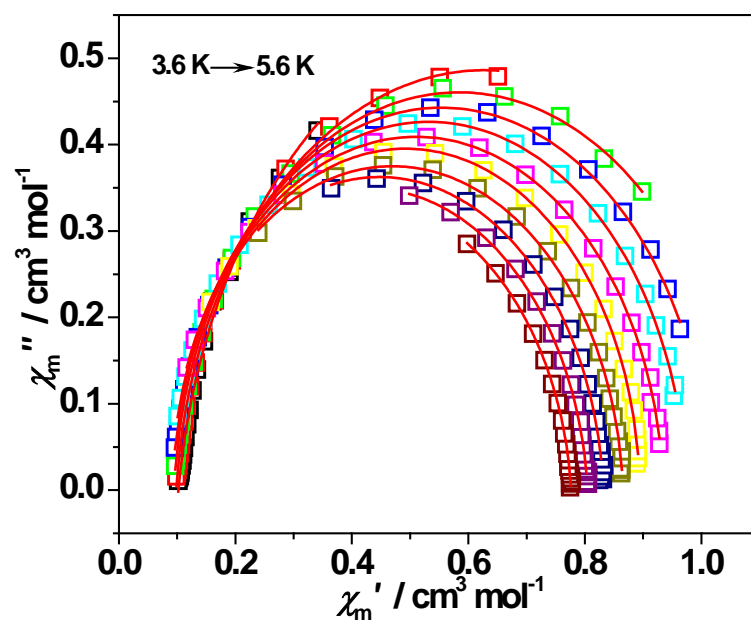


Fig. S7 Cole-Cole plots fitted by utilizing generalized Debye model for **2Er**. (a) presents the data from MPMS in the frequency range of 1-1000 Hz. (b) represents the data from PPMS in the frequency range of 100-10000 Hz.

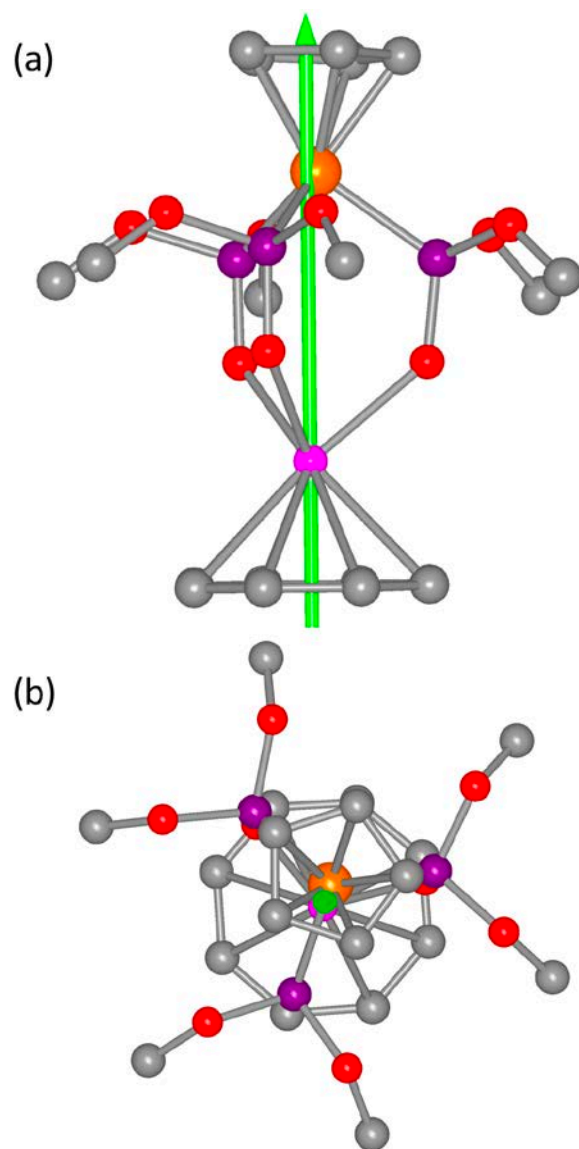


Fig. S8 *Ab initio* calculated easy axis for **1Er**.

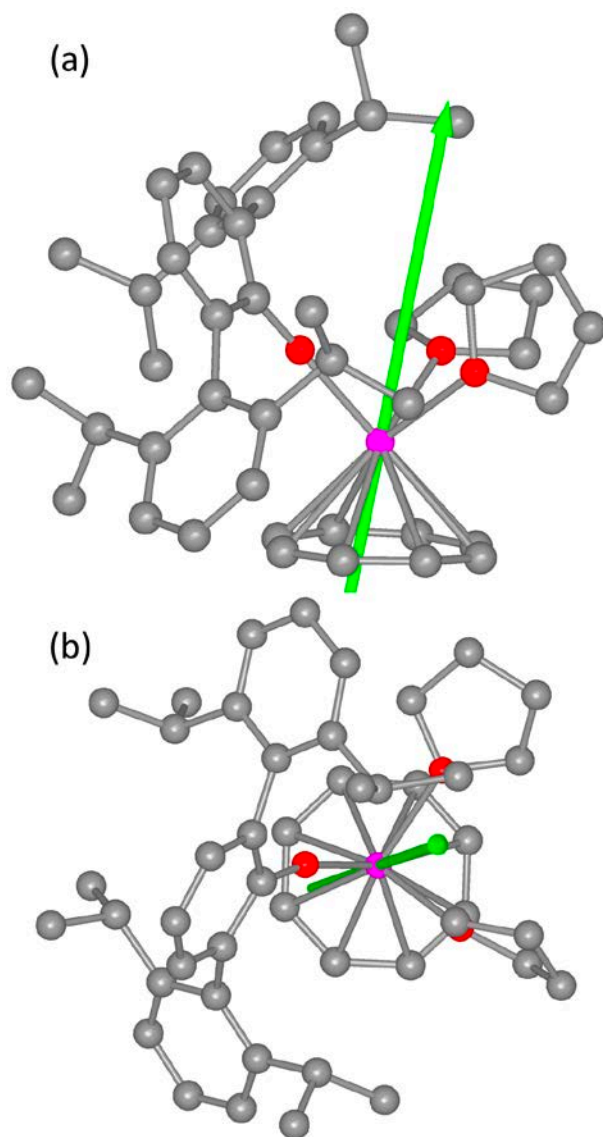


Fig. S9 *Ab initio* calculated easy axis for **2Er**.

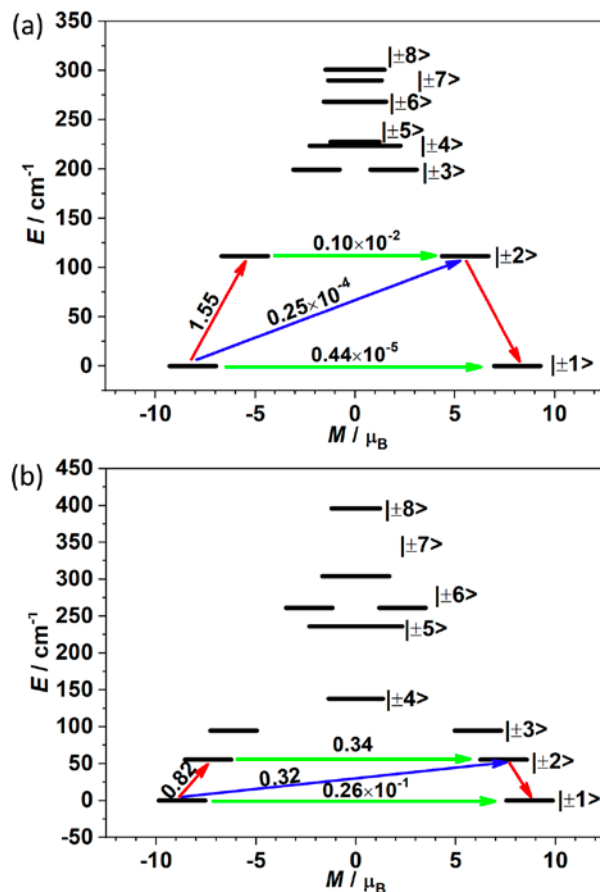


Fig. S10 The blocking barriers for 1Er (a) and 2Er (b). The thick black lines represent the exchange Kramer's doublets as a function of their magnetic moment along the magnetic axis. The green lines correspond to diagonal quantum tunneling of magnetization (QTM), the blue lines represent off-diagonal relaxation process. The numbers at each arrow stand for the mean absolute value of the corresponding matrix element of transition magnetic moment.

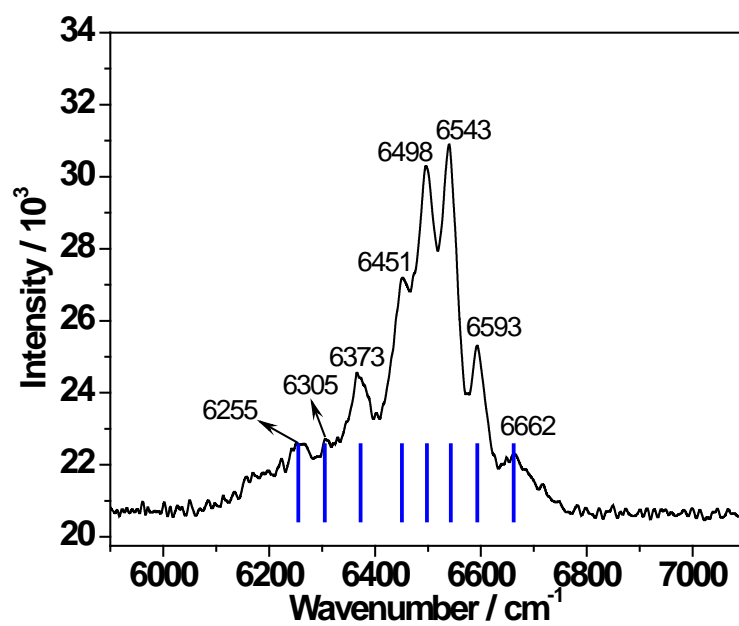


Fig. S11 Near-IR emissive spectra of **1Er** at 77 K. The blue lines represented the position the emissive peaks.